Ionization-induced effects in the soliton dynamics of high-peak-power femtosecond pulses in hollow photonic-crystal fibers

E. E. Serebryannikov and A. M. Zheltikov
Physics Department, International Laser Center, M.V. Lomonosov Moscow State University, Vorob'evy gory, Moscow 119992, Russia
(Received 15 March 2007; published 20 July 2007)

Ionization phenomena are shown to modify the soliton propagation dynamics of high-peak-power laser pulses in hollow-core photonic-crystal fibers (PCFs). Based on the numerical solution of the pulse-evolution equation for a high-peak-power laser field in an ionizing gas medium in a hollow PCF, we demonstrate that hollow PCFs filled with gases having high ionization potentials I_p can support soliton transmission regimes for gigawatt femtosecond laser pulses. In hollow PCFs filled with low-I_p gases, on the other hand, the ionization-induced change in the refractive index of the gas leads to a blueshifting of soliton transients, pushing their spectrum beyond the point of zero group-velocity dispersion, thus preventing the formation of stable high-peak-power solitons.

DOI: 10.1103/PhysRevA.76.013820 PACS number(s): 42.65.Wi

I. INTRODUCTION

Through the past few years, hollow-core photonic-crystal fibers (PCFs) [1,2] have emerged as an interesting type of optical waveguides, offering much promise for high-field physics and nonlinear optics. Diffraction-induced radiation losses, typical of hollow waveguides [3], can be substantially reduced in hollow PCFs due to the high reflectivity of a two-dimensionally periodic cladding within photonic band gaps (PBGs) [1,2,4–6]. Hollow PCFs offer a fiber format of high-power beam delivery in materials processing and related technologies [7,8] and suggest solutions for the development of advanced fiber-laser sources of ultrashort pulses [9–12], fiber microendoscopes [13,14], and other fiber-based components for biomedical applications [15]. Fibers of this type open new horizons in optical science by allowing guided-wave nonlinear-optical interactions of nondiverging laser beams with transverse sizes of a few microns—a unique regime of nonlinear optics that could not be accessed with previously known optical waveguides [16]. Large propagation lengths, phase-matching management through PCF structure engineering, and high peak powers of laser fields attainable with small-core hollow PCFs suggest attractive strategies toward a radical enhancement of a variety of nonlinear-optical processes, such as stimulated Raman scattering [17,18], off-resonance four-wave mixing [19,20], and coherent anti-Stokes Raman scattering [21,22]. The spatial self-action of intense ultrashort laser pulses gives rise to interesting waveguiding regimes in hollow PCFs below the beam blowup threshold [23].

In the regime of anomalous dispersion, the temporal self-action of laser pulses guided in the hollow core of PCFs can lead to the formation of solitons. While in standard optical fibers, the peak power of an individual (fundamental) soliton with a typical pulse width of 100 fs is usually on the order of a hundred watts; the peak power of solitons that can be produced in hollow PCFs can be as high as a few megawatts [24]. Soliton phenomena in hollow PCFs permit compression of high-peak-power laser pulses [25], allow the creation of wavelength-tunable high-peak-power fiber sources for nonlinear spectroscopy [26], and enable attractive regimes of long-distance transmission for high-power ultrashort laser pulses [27]. Skryabin *et al.* [28] have predicted the existence of two-color solitons in hollow PCFs filled with a Raman-active gas.

The main physical factors that limit the power of solitons in hollow PCFs include ionization of the gas filling the fiber core and the laser damage of the fiber cladding. We demonstrate in this work that, with an appropriate design of a hollow PCF, the peak power of fundamental solitons guided in the hollow core of such a fiber can be scaled up to several gigawatts. Ionization phenomena, on the other hand, will be shown to modify the soliton propagation dynamics of high-peak-power laser pulses in hollow-core PCFs. Numerical solution of a pulse-propagation equation for a high-peak-power laser field in an ionizing gas medium reveals two qualitatively different scenarios of soliton evolution in a hollow PCF, controlled by the ionization potential I_p of the gas filling the fiber core. Hollow PCFs filled with high-I_p gases are shown to allow the formation of gigawatt soliton features, which remain stable over large propagation distances, with their spectrum undergoing a continuous redshift due to the retarded nonlinearity of the fiber cladding and, in the case of Raman-active gases, due to the Raman effect in the gas. In hollow PCFs filled with low-I_p gases, the ionization-induced change in the refractive index of the gas leads to a blueshifting of soliton transients, pushing their spectrum beyond the point of zero group-velocity dispersion, thus preventing the formation of stable high-peak-power solitons.

II. MODELING PROPAGATION DYNAMICS OF HIGH-PEAK-POWER FEMTOSECOND PULSES IN A HOLLOW PCF FILLED WITH AN IONIZING GAS

To analyze the spectral and temporal evolution of a high-peak-power ultrashort pulse in a gas-filled hollow PCF, we work in the framework of the slowly evolving wave approximation (SEWA) [29,30]. In the earlier work on filamentation and supercontinuum generation in the atmosphere [31–34], the basic SEWA equations have been adapted to the description of high-intensity short laser pulses propagating in ionizing gas media [35–40]. While the evolution of high-intensity

laser fields in an ionizing atmosphere is usually analyzed with the dispersion profile of the medium included through a third-order polynomial expansion of the wave number in the frequency [40], thus accounting for dispersion effects up to the third order, an adequate description of the dispersion of hollow PCFs typically requires the inclusion of higher-order dispersion terms. In particular, a satisfactory fit for the dispersion profiles of hollow PCFs considered in this work is provided with a sixth-order polynomial. We therefore have to include dispersion effects up to the sixth order in our model.

Another important modification of pulse-evolution equations used throughout this work with respect to the equations employed to describe pulse propagation dynamics accompanying filamentation and supercontinuum generation in the atmosphere is related to the composite nature of optical nonlinearity of hollow PCFs, where both the gas filling the fiber core and the cladding material contribute to the instantaneous (Kerr-type) and retarded (Raman-type) parts of the overall nonlinear-optical response [41]. Since we consider here the propagation of laser fields in spatial modes of a hollow PCF with stationary transverse field profiles $F(x,y)$, where x and y are the transverse coordinates, we omit the terms governing the spatial dynamics of the laser field in the field-evolution equation. Instead, the nonlinear coefficients in our pulse-evolution equation are renormalized to include the transverse field profiles $F(x,y)$ in waveguide modes in accordance with the standard procedure [42,43], as specified in the nomenclature below. The resulting pulse-evolution equation for the field envelope $A(z,\tau)$ considered as a function of the propagation coordinate z and the retarded time τ reads

$$\begin{aligned}\frac{\partial A(z,\tau)}{\partial z} = & -\frac{1}{2}\left[\alpha + \frac{I_p}{I(z,\tau)}\frac{\partial n_e(z,\tau)}{\partial \tau}\right]A(z,\tau) \\ & - \sum_{m=2}^{6} \frac{i^{m+1}}{m!}\beta_m \frac{\partial^m A}{\partial \tau^m} + i\gamma_{\text{core}}\left(1 + \frac{i}{\omega_0}\frac{\partial}{\partial \tau}\right)A(z,\tau) \\ & \times \int_{-\infty}^{\tau} R_{\text{core}}(\theta)|A(z,\tau-\theta)|^2 d\theta \\ & + i\gamma_{cl}\left(1 + \frac{i}{\omega_0}\frac{\partial}{\partial \tau}\right)A(z,\tau) \\ & \times \int_{-\infty}^{\tau} R_{cl}(\theta)|A(z,\tau-\theta)|^2 d\theta - ik_0\frac{[\omega_p(z,\tau)]^2}{2\omega_0^2} \\ & \times A(z,\tau-\theta), \end{aligned} \tag{1}$$

where α is the attenuation coefficient, which includes the waveguide loss, I_p is the ionization potential, I (z, τ) is the field intensity, n_e is the electron density, $\beta_m = (\partial^m \beta/\partial \omega^m)_{\omega=\omega_0}$, β is the propagation constant of the waveguide mode, ω_0 is the central frequency of the laser field, $R_{\text{core}}(\theta)$ and $R_{cl}(\theta)$ are the Raman response functions of the gas filling the fiber core and the material of the fiber cladding, $k_0 = \omega_0/c$ is the wave number, $\omega_p(z,\tau) = [4\pi e^2 n_e(z,\tau)/m_e/]^{1/2}$ is the plasma frequency, e and m_e being the electron charge and mass, respectively.

The nonlinearity coefficients of the core and the cladding are defined as

$$\gamma_{\text{core}} = \frac{2\pi}{\lambda}\frac{n_{2g}\iint_{\Sigma_{\text{core}}} |F(x,y)|^4 dxdy}{\left[\iint_{\Sigma_\infty} |F(x,y)|^2 dxdy\right]^2}, \tag{2}$$

$$\gamma_{cl} = \frac{2\pi}{\lambda}\frac{n_{2cl}\iint_{\Sigma_{cl}} |F(x,y)|^4 dxdy}{\left[\iint_{\Sigma_\infty} |F(x,y)|^2 dxdy\right]^2}, \tag{3}$$

where n_{2g} and n_{2cl} are the nonlinear refractive indices of the gas filling the fiber core and the material of the fiber cladding, Σ_{core} and Σ_{cl} are the core and the cladding domains, respectively, Σ_∞ is the infinite domain, and λ is the radiation wavelength. With ionization terms omitted and the nonlinearity of the cladding neglected, Eq. (1) recovers the standard generalized nonlinear Schrödinger equation for pulse dynamics in optical fibers [43–45].

Qualitatively, the influence of ionization phenomena on pulse-propagation dynamics in a hollow PCF filled with an ionizing gas can be explained in terms of the following simplified arguments [46,47]. With an intensity of a laser pulse being high enough to ionize the gas, free electrons generated as a result of this ionization process reduce the refractive index of the gas medium at the frequency ω_0 by $\delta n_p(t) \approx -[\omega_p(t)]^2/(2\omega_0^2)$, where $\omega_p(t) = [4\pi e^2 n_e(t)/m_e]^{1/2}$ is the plasma frequency, e and m_e are the electron charge and mass, respectively, and $n_e(t)$ is the density of free electrons produced by the laser pulse. In Fig. 1, we plot the time dependence of δn_p calculated as a function of time by solving the relevant kinetic equation for the electron density $\partial n_e/\partial t = Wn$, where W is the ionization probability and n is the density of neutral species, and using the standard expressions for the ionization probability W in the multiphoton and tunneling regimes [48,49] (see [39,40] for a review) in the field of a 50 fs laser pulse (shown by the dashed line in Fig. 1) for laser field intensities varying from 2.7×10^{13} to 5.0×10^{13} W/cm^2. Since the time-dependent electron density $n_e(t)$ monotonically increases as long as the short-pulse laser field is on, $\delta n_p(t)$ is also a monotonic function of time, leading to a monotonic decrease in the refractive index of the gas in the course of the laser pulse and inducing a phase shift of the laser pulse $\varphi_p(t) = \omega_0 l \delta n_p(t)/c$, where l is the length of the ionizing gas medium and c is the speed of light. The time-dependent phase shift gives rise to a frequency shift of the laser pulse, $\delta\omega_p \approx -\partial\varphi_p(t)/\partial t = -(\omega_0 l/c)\partial[\delta n_p(t)]/\partial t$. As the electron density $n_e(t)$ monotonically increases within the laser pulse, $\partial[\delta n_p(t)]/\partial t < 0$ as long as the laser field is on (Fig. 1). Thus, the ionization-induced time-dependent change in the refractive index of a gas medium translates in a blueshift of the laser pulse, $\delta\omega_p > 0$.

The above-outlined simple scenario of blueshifting has been identified in earlier work on the dynamics and spectral

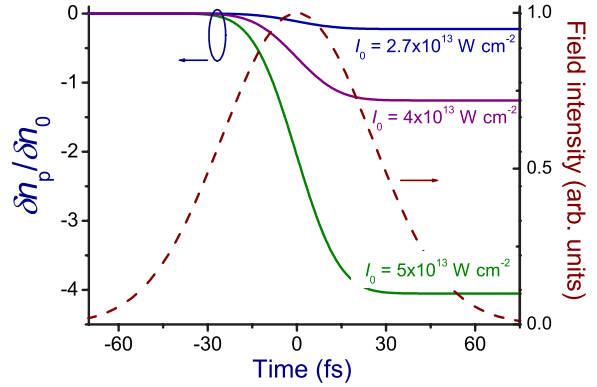

FIG. 1. (Color online) Ionization-induced change in the refractive index δn_p of an atmospheric-pressure air in the field of a laser pulse (shown by the dashed line) with a pulse width of 60 fs and peak intensities of 2.7×10^{13} W cm^{-2}, 4.0×10^{13} W cm^{-2}, and 5.0×10^{13} W cm^{-2}. The normalization constant δn_0 is defined as the absolute value of the ionization-induced change in the refractive index of an atmospheric-pressure air at the trailing edge of a 60 fs laser pulse with a peak intensity of 3.6×10^{13} W cm^{-2}.

transformations of high-intensity laser pulses in ionizing gas media [46]. In the waveguide regime, as shown below in this paper, this effect may lead to interesting and significant consequences, competing with a redshift of optical solitons induced by the Raman effect and giving rise to a net blueshifting of high-peak-power solitonic features of the laser field.

III. SOLITON DYNAMICS OF HIGH-PEAK-POWER PULSES IN A HOLLOW PCF FILLED WITH A RAMAN-ACTIVE GAS

We start our analysis with the dynamics of pulse propagation in a hollow PCF with a core diameter of 13 μm and a period of the photonic-crystal cladding of 5 μm. The dispersion profile for this fiber is shown in Fig. 2. Hollow PCFs of this and similar types have been earlier used for the experimental demonstration of high-peak-power solitons and enhance nonlinear-optical interactions of laser pulses within a broad range of pulse widths [2,5,6,8,26,41]. The considered type of PCF provides a transmission band in the range of wavelengths from 775 to 855 nm with a waveguide loss of 2 dB/m at the maximum of transmission. Typically of hollow PCFs, the spectral profile of the group-velocity dispersion (GVD) is flat inside the transmission band, but becomes very steep near the edges of this band, where the reflection from the photonic-crystal cladding rapidly drops off and the phase shift induced by the reflection from the core-cladding interface is a rapidly changing function of frequency. The considered type of PCFs, as can be seen from Fig. 2, provides anomalous dispersion within the wavelength range from 787 nm (the point of zero GVD) up to 855 nm (the long-wavelength edge of the transmission band of the PCF).

Here, we assume that, similar to experiments reported in [24,26,41], the fiber is filled with atmospheric-pressure air and solve Eq. (1) with the Raman function of atmospheric air used as R_{core} and the standard Raman function of silica used as R_{cl} as follows:

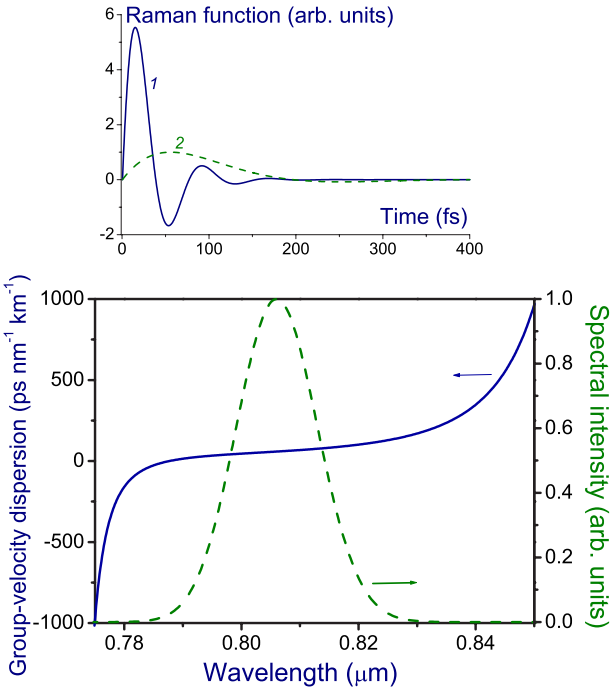

FIG. 2. (Color online) Group-velocity dispersion (solid line) as a function of the wavelength for a hollow-core PCF with a core diameter of 13 μm and a period of the photonic-crystal cladding of 5 μm. Also shown is the spectrum of a femtosecond Ti:sapphire laser pulses used as a PCF input (dashed curve). The inset shows the Raman functions of the silica cladding of PCF (1) and atmospheric air filling the fiber core (2).

$$R_{\text{core},cl}(\theta) = (1 - f_{1,2})\delta(\theta) + f_{1,2}\Theta(\theta)\frac{\tau_{1,2}^2 + \eta_{1,2}^2}{\tau_{1,2}\eta_{1,2}^2} e^{-\theta/\eta_{1,2}} \sin\left(\frac{\theta}{\tau_{1,2}}\right), \quad (4)$$

where f_i is the fractional contribution of the Raman response, $\delta(\theta)$ and $\Theta(\theta)$ are the delta and the Heaviside step functions, respectively, τ_i and η_i are the characteristic times of the Raman response, and $i=1,2$ for the core and the cladding, respectively. For a hollow PCF filled with atmospheric air, $f_1 \approx 0.5$, $\tau_1 \approx 62.5$ fs, and $\eta_1 \approx 77$ fs. For a fused silica PCF cladding, $f_2 \approx 0.18$, $\tau_2 \approx 12.5$ fs, and $\eta_2 \approx 32$ fs. The Raman response functions for the atmospheric air and fused silica are shown in the inset to Fig. 2.

Figures 3 and 4 illustrate two representative scenarios of pulse-propagation dynamics in the regime of anomalous dispersion in the considered PCF for a laser field with an input spectrum shown by the dashed line in Fig. 2 and two different input peak powers. In Fig. 3, we present the temporal evolution of a laser pulse with an input peak power of 2.3 MW. For the fundamental waveguide mode of the considered PCF, these parameters of the input pulse correspond to a field intensity of 3.0×10^{12} W/cm^2. Such a field intensity is too low to produce a noticeable electron density in the gas filling the fiber core (see Fig. 1), and the influence of ionization effects on pulse-propagation dynamics is negligible. The input peak power of laser pulses, at the same time, is too low for the formation of solitons. As a result, although

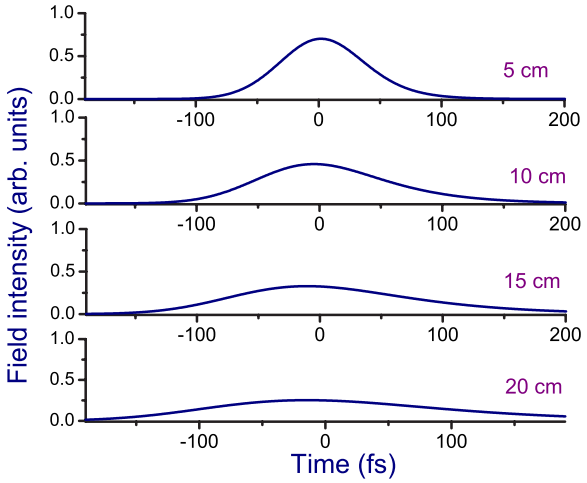

FIG. 3. (Color online) Temporal dynamics of a laser pulse propagating in a hollow PCF filled with an atmospheric-pressure gas. The input peak power is 2.3 MW. The input spectrum of the laser field is shown by the dashed line in Fig. 2.

the input spectrum of the laser field falls within the range of anomalous dispersion (Fig. 2), the laser pulse, as can be seen in Fig. 3, undergoes a PCF-dispersion-induced spreading in the time domain as it propagates down the fiber. Within 20 cm of PCF, the pulse width increases in this regime from 50 fs at the input of the fiber to approximately 200 fs.

Input laser pulses with a higher input peak power tend to form solitons as they propagate through the PCF in the regime of anomalous dispersion. This type of pulse-propagation dynamics is illustrated by Figs. 4(a) and 4(b), representing the results of simulations performed for an input laser pulse with an input spectrum shown by the dashed line in Fig. 2 and a peak power of 31 MW, corresponding to the field intensity of 4.0×10^{13} W/cm^2 in the fundamental mode of the considered fiber. In this regime, the solitonic dynamics suppresses the spreading of the laser field in the time domain [Fig. 4(a)]. At the initial stage of pulse propagation (within approximately 6 cm in the case considered here), the laser field undergoes solitonic pulse compression. This effect increases the peak intensity of the laser field by a factor of about 1.5, enhancing ionization of the gas filling the fiber core. As a result, the laser field experiences a noticeable blueshifting, as shown by the snapshot of the field spectrum corresponding to the propagation distance $z=6$ cm in Fig. 4(b). As the pulse propagates further on along the fiber, it loses its energy through ionization and because of waveguide loss, which tends to increase as the field spectrum is shifted toward the short-wavelength edge of the transmission band. These effects arrest the spectral blueshifting of the laser field, leading to the domination of the Raman-effect-induced redshifting of solitonic features (soliton self-frequency shift [43,50,51]) for larger propagation lengths [$z>9$ cm in Fig. 4(b)].

IV. DESIGNING A HOLLOW PCF FOR THE TRANSMISSION OF GIGAWATT FEMTOSECOND PULSES

We now proceed with the analysis of soliton-propagation dynamics for laser fields in the gigawatt range of peak pow-

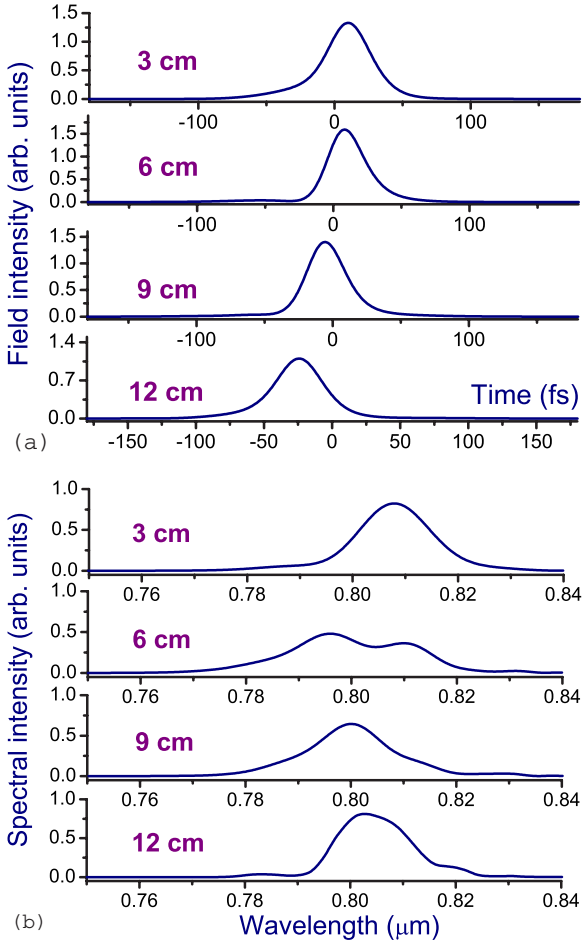

FIG. 4. (Color online) Temporal (a) and spectral (b) dynamics of a laser pulse propagating in a hollow PCF filled with an atmospheric-pressure gas. The input peak power is 31 MW. The input spectrum of the laser field is shown by the dashed line in Fig. 2.

ers. In designing waveguide structures for the transmission of such laser fields, special precautions should be taken to avoid laser damage of the fiber cladding. Mathematically, the requirement of no laser-induced damage in the fiber cladding is formalized by the inequality

$$\max_{\Sigma}\{G(x,y)\} < G_{th}, \tag{5}$$

where G_{th} is the threshold fluence corresponding to the laser damage of the cladding material, $G(x,y)$ is the local fluence at a point with coordinates (x,y) in PCF cross section, and $\max_{\Sigma}\{G(x,y)\}$ stands for the global maximum of $G(x,y)$ over the entire PCF cross-section area Σ.

An idealized PCF structure satisfying condition (5) is presented in inset 1 to Fig. 5. Dispersion and loss, as well as transverse field profiles for the waveguide modes of this PCF were analyzed numerically using the localized-function technique described in detail elsewhere [22,52]. A large fiber core of the considered PCF (its diameter is equal to 30 μm, and the effective area of the fundamental waveguide mode is about 380 μm^2) helps to accommodate high-peak-power la-

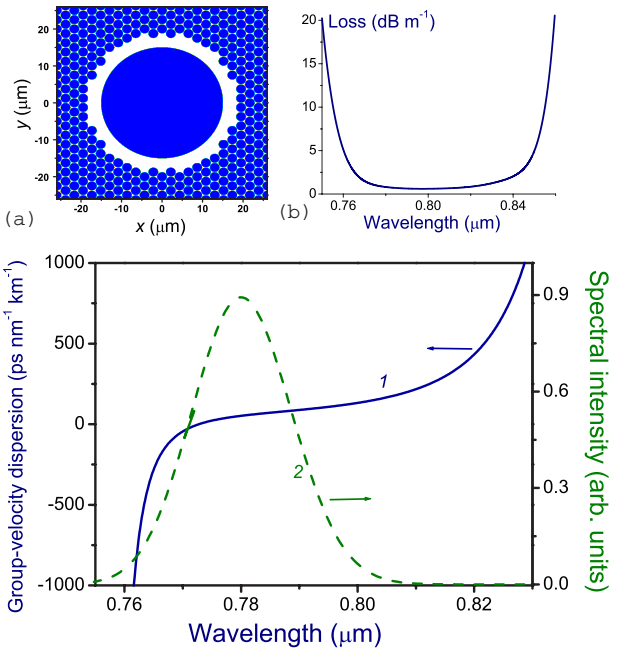

FIG. 5. (Color online) The group-velocity dispersion as a function of the wavelength for the hollow PCF shown in inset (a) (solid line 1) and the input spectrum of the laser pulse used in simulations (dashed line 2). Inset (b) displays the waveguide loss for the fundamental mode of the hollow PCF as a function of the wavelength.

ser pulses, reducing the fraction of the total radiation power guided along the fiber-cladding laser energy. The fiber provides a transmission band in the range of wavelengths from 760 to 845 nm (inset 2 in Fig. 5). For laser pulses with an input peak power of 3 GW and an initial pulse width of 50 fs coupled into the fundamental mode of the considered fiber, our numerical simulations yield $\max_{\Sigma}\{G(x,y)\} \approx 0.6\ \mathrm{J/cm^2}$. Such a fluence is lower than the threshold fluence for bulk silica ($G_{th} \approx 3\ \mathrm{J/cm^2}$ for 800 nm, 50 fs laser pulses), and no laser damage of the fiber cladding is expected for the regime of the established guided mode.

Figure 5 displays the wavelength dependence of the group-velocity dispersion (GVD) for the fundamental mode of the considered type of hollow PCF. The GVD is anomalous for radiation wavelengths exceeding the zero-GVD wavelength $\lambda_z \approx 770$ nm. This fiber is thus ideally suited for a low-loss transmission of femtosecond high-peak-power Ti:sapphire laser pulses in the anomalous dispersion regime (shown by the dashed line in Fig. 5). The spectral and temporal dynamics of such pulses in the considered type of PCF will be examined in the following section.

V. SOLTION DYNAMICS OF GIGAWATT LIGHT PULSES IN A HOLLOW PCF FILLED WITH A RARE GAS

As the intensity of the laser field increases, ionization effects play a progressively important role in the dynamics of pulse propagation in an ionizing gas medium. For a given level of laser intensity, however, the ionization probability may vary within a broad range, depending on the ionization potential I_p of an atom or a molecule. To understand the influence of this parameter on the soliton dynamics of high-peak-power laser pulses in hollow PCFs, we consider fibers filled with three different rare gases—argon, helium, and neon. These gases are a common choice for hollow-waveguide high-field laser experiments as they do not react with the walls of the waveguide and are safe and predictable with respect to interactions with high-intensity laser radiation and plasma formation. Methodologically, since these gases are not active in Raman scattering, they allow us to isolate ionization-induced effects from the redshift of laser pulses related to the Raman part of nonlinear-optical response. It should be noted here that, because of the Raman nonlinearity of the fiber cladding, the Raman-effect-induced soliton frequency shifts in hollow PCFs cannot be completely eliminated even with rare gases filling the fiber core.

In Figs. 6(a)–6(c), we plot the time dependence of the ionization-induced change in the refractive index δn_p of argon, helium, and neon at three different pressures calculated as a function of time by solving the relevant kinetic equation for the electron density and using the standard expressions for the ionization probability in the multiphoton and tunneling regimes in the field of a 50-fs laser pulse (shown by the dashed line) with a peak power of 3 GW. Comparison of these results shows that, for given parameters of a laser pulse, the most significant ionization effects in pulse-propagation dynamics should be expected in the case of argon [Fig. 6(c)], where the ionization potential is lowest ($I_p \approx 15.75$ eV), leading to the largest change in the refractive index. In helium, on the other hand, where the ionization potential is much higher ($I_p \approx 24.58$ eV), the refractive index change δn_p is much smaller [Fig. 6(a)], leading to much less dramatic ionization effects in pulse-propagation dynamics.

Numerical simulations of the spectral and temporal dynamics of gigawatt femtosecond laser pulses propagating in hollow PCFs filled with rare gases were performed for low gas pressures, ranging from 0.01 to 0.03 atm, which helped us to avoid uncontrollable plasma effects. Gas pressures are also typically kept low in experiments where hollow waveguides are used to compress high-intensity laser pulses or to generate high-order optical harmonics. At this level of gas pressures, the nonlinearity of the fiber cladding often dominates the overall nonlinearity of the hollow PCF. For example, in the case when a hollow PCF with a transverse structure shown in inset 1 to Fig. 5 is filled with argon at a pressure of 0.01 atm, the ratio $\gamma_{cl}/\gamma_{\mathrm{core}}$ is estimated as 40.

For hollow PCFs filled with low-I_p gases, such as Ar, ionization leads to a strong blueshift of the pulse [the dashed line in Figs. 7(a) and 7(b)]. Under these conditions, the field loses much of its energy through gas ionization. At the same time, the ionization-induced blueshift rapidly pushes the spectrum of the field beyond the zero-GVD point into the region of normal dispersion [$z=1$ cm in Fig. 7(b)], where the pulse undergoes a fast temporal spreading [Fig. 7(a)], losing its intensity.

In the case of a hollow PCF filled with high-I_p gases, such as helium, the influence of ionization effects is much less dramatic [the solid line in Figs. 7(a) and 7(b)]. In this case, following the initial stage of spectral broadening, the laser field undergoes a series of transformations typical of a short

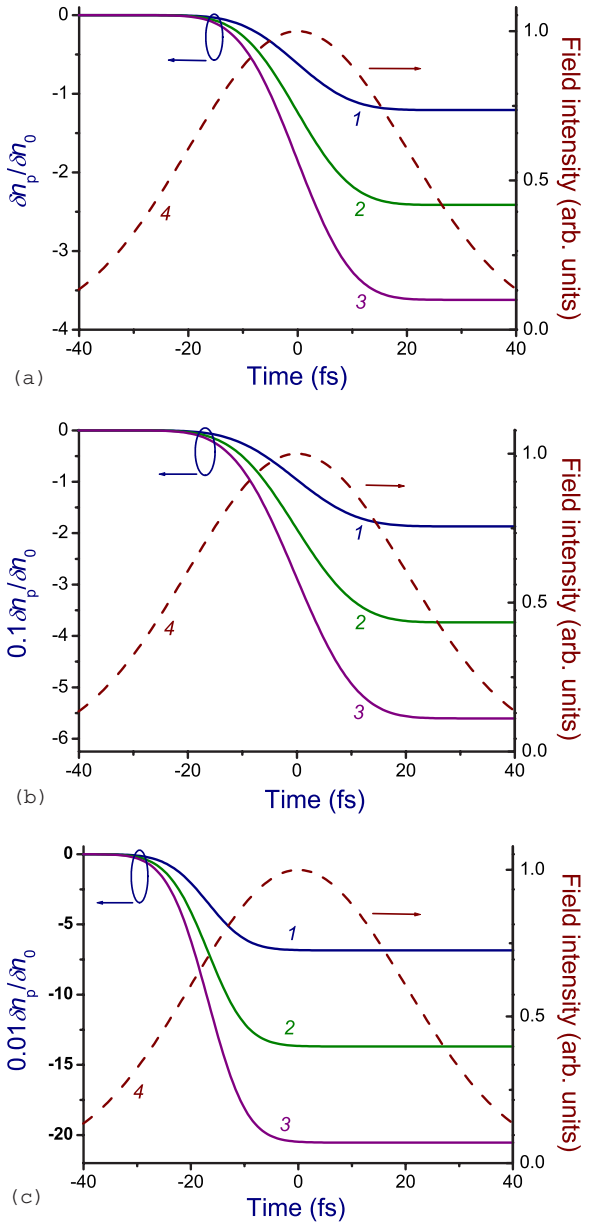

FIG. 6. (Color online) Ionization-induced change in the refractive index of (a) helium, (b) neon, and (c) argon at a pressure of (1) 0.01 atm, (2) 0.02 atm, and (3) 0.03 atm in the field of a laser pulse (shown by dashed line 4) with a pulse width of 50 fs and a peak power of 3 GW. The normalization constant δn_0 is defined as the absolute value of the ionization-induced change in the refractive index of an atmospheric-pressure air at the trailing edge of a 60 fs laser pulse with a peak intensity of 3.6×10^{13} W cm^{-2}.

laser pulse propagating in a nonlinear fiber close to the zero-GVD wavelength, as identified in the classical texts on fiber nonlinear optics. The spectrum of the laser field in this regime splits into two parts [Fig. 7(b)] with a depletion of the central part of the spectrum, lying close to the zero-GVD wavelength. The long-wavelength part of the field spectrum falls within the region of anomalous dispersion, giving rise to a soliton, which undergoes redshifting due to the Raman part of optical nonlinearity in the fiber cladding.

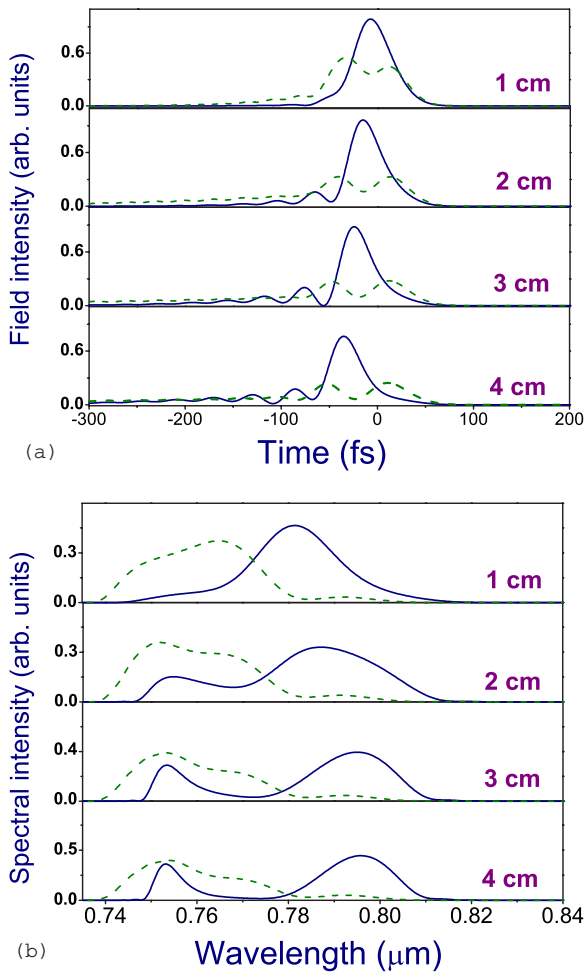

FIG. 7. (Color online) Temporal (a) and spectral (b) dynamics of a laser pulse propagating in a hollow PCF filled with helium (solid line) and argon (dashed line) at a pressure of 0.01 atm. The input pulse peak power is 2 GW. The initial pulse width is 50 fs.

Hollow PCFs filled with high-I_p gases thus allow transmission of solitons in the gigawatt range of peak powers with minimal distortions induced by ionization effects. In Figs. 8(a) and 8(b), we illustrate this interesting and practically significant regime of high-power pulse waveguide transmission by presenting the spectral and temporal evolution of laser pulses with an input peak power of 3 GW and an initial pulse width of 50 fs in the considered type of hollow PCF filled with helium and neon at a pressure of 0.03 atm. In this regime, the field spectrum is also split into two parts, with its central part lying close to the zero-GVD wavelength being depleted [Fig. 8(b)]. The long-wavelength part of the field falls in the range of anomalous dispersion, giving rise to prominent high-peak-power solitonic features in the time domain [Fig. 8(a)]. As the ionization potential of neon ($I_p \approx 21.52$ eV) is lower than the I_p of helium, the solitonic part of the field in a neon-filled PCF experiences a more pronounced blueshift than the solitonic features formed in a helium-filled PCF [cf. the solid and dashed curves in Fig. 8(b)]. For the nonsolitonic part of the field [the shorter wavelength peaks in Fig. 8(b)], the blueshift is much less significant because this part of the field experiences temporal

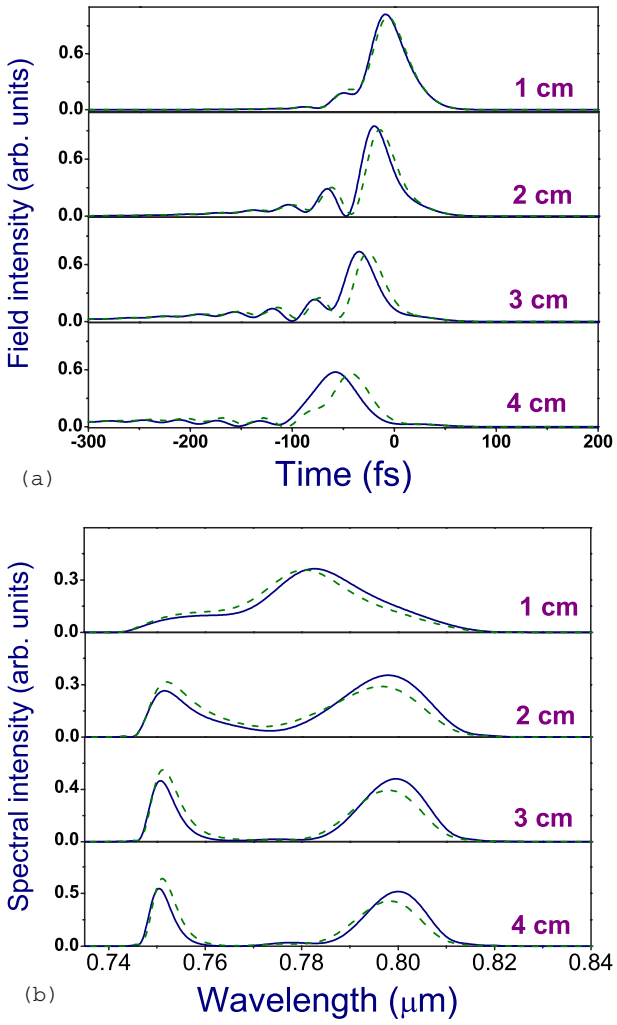

FIG. 8. (Color online) Temporal (a) and spectral (b) dynamics of a laser pulse propagating in a hollow PCF filled with helium (solid line) and neon (dashed line) at a pressure of 0.03 atm. The input pulse peak power is 3 GW. The initial pulse width is 50 fs.

spreading and its intensity is much lower than the intensity of the solitonic part of the field.

VI. CONCLUSION

We have shown in this paper that ionization phenomena can substantially modify the soliton propagation dynamics of high-peak-power laser pulses in hollow-core PCFs. Numerical solution of the pulse-evolution equation for a high-peak-power laser field in an ionizing gas medium reveals two qualitatively different scenarios of soliton evolution in a hollow PCF controlled by the ionization potential I_p of the gas filling the fiber core. Hollow PCFs filled with high-I_p gases are shown to allow formation of gigawatt soliton features, which remain stable over large propagation distances, with their spectrum undergoing a continuous redshift due to the retarded nonlinearity of the fiber cladding. In hollow PCFs filled with low-I_p gases, the ionization-induced change in the refractive index of the gas leads to a blueshifting of soliton transients, pushing their spectrum beyond the point of zero group-velocity dispersion, thus preventing formation of stable high-peak-power solitons. Hollow waveguides capable of providing soliton transmission regimes for gigawatt laser pulses suggest attractive solutions for long-distance transmission of high-power optical signals, creation of wavelength-tunable sources of high-peak-power ultrashort light pulses, fiber-format beam delivery in materials microprocessing, as well as the development of fiber endosopes and fiber components for laser surgery, vessel photodisruption, laser ophthalmology, and optical histology.

ACKNOWLEDGMENTS

Useful discussions with Yu.M. Mikhailova are gratefully acknowledged. This study was supported in part by the Russian Foundation for Basic Research (Projects No. 06-02-16880 and No. 05-02-90566-NNS) and INTAS (Projects No. 03-51-5037 and No. 03-51-5288). The research described in this publication was made possible by the U.S. Civilian Research & Development Foundation for the Independent States of the Former Soviet Union (CRDF).

[1] R. F. Cregan, B. J. Mangan, J. C. Knight, T. A. Birks, P. St. J. Russell, P. J. Roberts, and D. C. Allan, Science **285**, 1537 (1999).
[2] P. St. J. Russell, Science **299**, 358 (2003).
[3] E. A. J. Marcatili and R. A. Schmeltzer, Bell Syst. Tech. J. **43**, 1783 (1964).
[4] S. O. Konorov, A. B. Fedotov, O. A. Kolevatova, V. I. Beloglazov, N. B. Skibina, A. V. Shcherbakov, and A. M. Zheltikov, JETP Lett. **76**, 341 (2002).
[5] C. M. Smith, N. Venkataraman, M. T. Gallagher, D. Muller, J. A. West, N. F. Borrelli, D. C. Allan, and K. Koch, Nature (London) **424**, 657 (2003).
[6] G. Bouwmans, F. Luan, J. C. Knight, P. St. J. Russell, L. Farr, B. J. Mangan, and H. Sabert, Opt. Express **11**, 1613 (2003).
[7] S. O. Konorov, A. B. Fedotov, O. A. Kolevatova, V. I. Beloglazov, N. B. Skibina, A. V. Shcherbakov, E. Wintner, and A. M. Zheltikov, J. Phys. D **36**, 1375 (2003).
[8] J. D. Shephard, J. D. C. Jones, D. P. Hand, G. Bouwmans, J. C. Knight, P. S. J. Russell, and B. J. Mangan, Opt. Express **12**, 717 (2004).
[9] J. Limpert, T. Schreiber, S. Nolte, H. Zellmer, and A. Tünnermann, Opt. Express **11**, 3332 (2003).
[10] C. J. S. de Matos, S. V. Popov, A. B. Rulkov, J. R. Taylor, J. Broeng, T. P. Hansen, and V. P. Gapontsev, Phys. Rev. Lett. **93**, 103901 (2004).
[11] X. Chen, M. Li, N. Venkataraman, M. T. Gallagher, W. A. Wood, A. M. Crowley, J. P. Carberry, L. A. Zenteno, and K. W. Koch, Opt. Express **12**, 3888 (2004).

[12] H. Lim, A. Chong, and F. W. Wise, Opt. Express **13**, 3460 (2005).
[13] B. Flusberg, J. Jung, E. Cocker, E. Anderson, and M. Schnitzer, Opt. Lett. **30**, 2272 (2005).
[14] L. Fu, A. Jain, H. Xie, C. Cranfield, and M. Gu, Opt. Express **14**, 1027 (2006).
[15] S. O. Konorov, A. B. Fedotov, V. P. Mitrokhin, V. I. Beloglazov, N. B. Skibina, A. V. Shcherbakov, E. Wintner, M. Scalora, and A. M. Zheltikov, Appl. Opt. **43**, 2251 (2004).
[16] A. M. Zheltikov, Phys. Usp. **47**, 1205 (2004).
[17] F. Benabid, J. C. Knight, G. Antonopoulos, and P. St. J. Russell, Science **298**, 399 (2002).
[18] F. Benabid, F. Couny, J. C. Knight, T. A. Birks, and P. St. J. Russell, Nature (London) **434**, 488 (2005).
[19] S. O. Konorov, A. B. Fedotov, and A. M. Zheltikov, Opt. Lett. **28**, 1448 (2003).
[20] S. O. Konorov, E. E. Serebryannikov, D. A. Akimov, A. A. Ivanov, M. V. Alfimov, and A. M. Zheltikov, Phys. Rev. E **70**, 066625 (2004).
[21] A. B. Fedotov, S. O. Konorov, V. P. Mitrokhin, E. E. Serebryannikov, and A. M. Zheltikov, Phys. Rev. A **70**, 045802 (2004).
[22] S. O. Konorov, E. E. Serebryannikov, A. B. Fedotov, R. B. Miles, and A. M. Zheltikov, Phys. Rev. E **71**, 057603 (2005).
[23] S. O. Konorov, A. M. Zheltikov, Ping Zhou, A. P. Tarasevitch, and D. von der Linde, Opt. Lett. **29**, 1521 (2004).
[24] D. G. Ouzounov, F. R. Ahmad, D. Müller, N. Venkataraman, M. T. Gallagher, M. G. Thomas, J. Silcox, K. W. Koch, and A. L. Gaeta, Science **301**, 1702 (2003).
[25] D. G. Ouzounov, C. J. Hensley, A. L. Gaeta, N. Venkateraman, M. T. Gallagher, and K. W. Koch, Opt. Express **13**, 6153 (2005).
[26] A. A. Ivanov, A. A. Podshivalov, and A. M. Zheltikov, Opt. Lett. **31**, 3318 (2006).
[27] F. Luan, J. C. Knight, P. St. J. Russell, S. Campbell, D. Xiao, D. T. Reid, B. J. Mangan, D. P. Williams, and P. J. Roberts, Opt. Express **12**, 835 (2004).
[28] D. V. Skryabin, F. Biancalana, D. M. Bird, and F. Benabid, Phys. Rev. Lett. **93**, 143907 (2004).
[29] T. Brabec and F. Krausz, Phys. Rev. Lett. **78**, 3282 (1997).
[30] A. L. Gaeta, Phys. Rev. Lett. **84**, 3582 (2000).
[31] A. Braun, G. Korn, X. Liu, D. Du, J. Squier, and G. Mourou, Opt. Lett. **20**, 73 (1995).
[32] E. T. Nibbering, P. F. Curley, G. Grillon, B. S. Prade, M. A. Franco, F. Salin, and A. Mysyrowicz, Opt. Lett. **21**, 1 (1996).
[33] B. La Fontaine, F. Vidal, Z. Jiang, C. Y. Chien, D. Comtois, A. Desparois, T. W. Johnston, J.-C. Kieffer, H. Pepin, and H. P. Mercure, Phys. Plasmas **6**, 1615 (1999).
[34] J. Kasparian, M. Rodriguez, G. M'ejean, J. Yu, E. Salmon, H. Wille, R. Bourayou, S. Frey, Y. B. Andre, A. Mysyrowicz, R. Sauerbrey, J. P. Wolf, and L. Woeste, Science **301**, 61 (2003).
[35] O. G. Kosareva, V. P. Kandidov, A. Brodeur, C. Y. Chien, and S. L. Chin, Opt. Lett. **22**, 1332 (1997).
[36] N. Akozbek, M. Scalora, C. M. Bowden, and S. L. Chin, Opt. Commun. **191**, 353 (2001).
[37] M. Mleinek, E. M. Wright, and J. V. Moloney, Opt. Lett. **23**, 382 (1998).
[38] M. Mlejnek, E. M. Wright, and J. V. Moloney, Phys. Rev. E **58**, 4903 (1998).
[39] P. Sprangle, J. R. Penano, and B. Hafizi, Phys. Rev. E **66**, 046418 (2002).
[40] V. P. Kandidov, O. G. Kosareva, I. S. Golubtsov, W. Liu, A. Becker, N. Akozbek, C. M. Bowden, and S. L. Chin, Appl. Phys. B: Lasers Opt. **77**, 149 (2003).
[41] I. V. Fedotov, A. B. Fedotov, and A. M. Zheltikov, Opt. Lett. **31**, 2604 (2006).
[42] Y. R. Shen, *The Principles of Nonlinear Optics* (Wiley, New York, 1984).
[43] G. P. Agrawal, *Nonlinear Fiber Optics* (Academic, San Diego, 2001).
[44] P. Beaud, W. Hodel, B. Zysset, and H. P. Weber, IEEE J. Quantum Electron. **23**, 1938 (1987).
[45] K. J. Blow and D. Wood, IEEE J. Quantum Electron. **25**, 2665 (1989).
[46] W. M. Wood, C. W. Siders, and M. C. Downer, Phys. Rev. Lett. **67**, 3523 (1991).
[47] A. B. Fedotov, N. I. Koroteev, M. M. T. Loy, X. Xiao, and A. M. Zheltikov, Opt. Commun. **133**, 587 (1997).
[48] L. V. Keldysh, Sov. Phys. JETP **20**, 1307 (1964).
[49] A. M. Perelomov, V. S. Popov, and M. V. Terent'ev, Sov. Phys. JETP **23**, 924 (1966).
[50] E. M. Dianov, A. Ya. Karasik, P. V. Mamyshev, A. M. Prokhorov, V. N. Serkin, M. F. Stel'makh, and A. A. Fomichev, JETP Lett. **41**, 294 (1985).
[51] F. M. Mitschke and L. F. Mollenauer, Opt. Lett. **11**, 659 (1986).
[52] L. Poladian, N. A. Issa, and T. M. Monro, Opt. Express **10**, 449 (2002).